Photoinduced Betaine Generation for the Efficient Photothermal Energy Conversion

Devika Sasikumar,[a] Yuta Takano,*[a,b] and Vasudevanpillai Biju*[a,b]

Abstract: The conversion of solar energy to thermal, chemical, or electrical energy attracts great attention in chemistry and physics. There has been a considerable effort for the efficient extraction of photons throughout the entire solar spectrum. In this study, we efficiently harvest light energy using a long-lived photogenerated betaine from an acridinium-based electron donor-acceptor dyad. The photothermal energy conversion efficiency of the dyad is significantly enhanced by the simultaneous illumination of blue (420-440 nm) and yellow (>480 nm) lights, which is when compared with the sum of independent blue and yellow light illuminations. The enhanced photothermal effect is due to the photogenerated betaine, which absorbs longer wavelength light than the dyad, making the dyad-betaine combination promising for efficient photothermal energy conversion. The mechanisms of betaine generation and energy conversion are discussed based on steady-state and transient spectral measurements.

Introduction

Exploring the full use of solar energy by photoexcitation of molecules has gained significant attention in versatile fields of physics, chemistry, and biology.[1-4] Representative state-of-art examples are photovoltaics,[1] artificial photosynthesis,[2] photocatalysis,[3] and phototherapy.[4] However, the utility and efficiency of molecular systems are often limited due to the usable classes of light. For instance, light-harvesting efficiency is limited by the structure of molecules that governs the absorption properties. Novel molecules and nanomaterials have been designed and employed for the efficient absorption and harvesting of the entire spectrum of solar energy.[5] The general approach to cover the solar spectrum is to extend the pi-conjugation structure in organic chromophores by employing chemical modification or novel synthesis, which is resource-demanding and tediously time-consuming.[6] Meanwhile, the use of the electronic structure of the photoexcited states of molecules or photogenerated species can be an alternative approach to harvest longer wavelength regions effectively. However, such approaches using organic molecules are limited and demands further attention.[7]

The photothermal conversion of light energy is one of the conventional approaches to energy harvesting.[8] The significance of this approach is still growing owing to the applications of photothermal energy to photocatalytic reactions, solar energy harvesting, and photoacoustic theragnosis.[9] An efficient photothermal agent exhibits strong light absorbance, substantial photothermal conversion efficiency, and robust photostability.[10] In this context, various classes of photothermal agents have been introduced, comprising nanomaterials and organic compounds[4d-e] Among them, organic photothermal agents are attractive owing to the features such as biocompatibility, and environment-friendliness.[10] Furthermore, the flexible structure of organic chromophores makes them appealing for various purposes.[4d] Although, one of the severe limitations during photon absorption is the decomposition of molecules shined with intense light, which may lead to low durability, hampering the practical application of the organic molecules.[11] Photodecomposition may occur as the result of undesired generations of reactive species or uncontrolled redox reactions at the photo-excited states.[12] Therefore, significant efforts have been dedicated to overcoming this problem, which is by designing rigid molecular frameworks or controlling the assembly at the molecular level.

In this study, we are reporting a novel approach to utilize a photogenerated species from a donor-acceptor linked molecule with high durability for the efficient use of light energy (Figure 1). As the molecular skeleton, we chose 9-position substituted acridinium moiety, which is intensively studied for photocatalysis and artificial photosynthesis due to the efficieny to form long-living charge-separated states.[2e,3a] We synthesized and examined acridinium-based molecules to utilize their excited state properties.In this work, the photothermal effect exhibited by an electron donor-acceptor dyad **1** is investigated and compared with two model compounds **2** (9-mesityl-10-methylacridinium chloride) and **3** (10-methylacridinium ion). Here, **1** shows photoinduced betaine generation with notably long lifetime. Additional illumination of **1** led to remarkable enhancement in photothermal effect (PTE) due to the extended absorption of the visible light by the long-lived photogenerated betaine. The photothermal generator, **1** showed excellent photostability irrespective of the pH of the aqueous medium. Betaine-type molecules predominantly prefer a nonradiative relaxation pathway to liberate the excitation energy, which leads to the high efficiency of PTE.[13] Also, 9-mesityl-10-methylacridinium ion has been extensively utilized as an efficient photocatalyst and as a molecule for photocontrolling biological activities.[3a, 14-16] However, the number of studies that report the photostability and recyclability of 9-mesityl-10-methylacridinium ions in aqueous solution are limited. One of the interesting facts revealed in the present study is pH-dependent photodecomposition 9-mesityl-10-methylacridinium ion, which would hamper the extensive practical application of the model compound **2** (9-mesityl-10-methylacridinium ion) in the aqueous medium.

[a] D. Sasikumar, Prof. Dr. Y. Takano, Prof. Dr. V. Biju
Graduate School of Environmental Science, Hokkaido University
N10, W5, Sapporo, 060-0810 (Japan)
E-mail: tak@es.hokudai.ac.jp, biju@es.hokudai.ac.jp
[b] Prof. Dr. Y. Takano, Prof. Dr. V. Biju,
Research Institute for Electronic Science, Hokkaido University
N20, W10, Sapporo, 001-0020 (Japan)

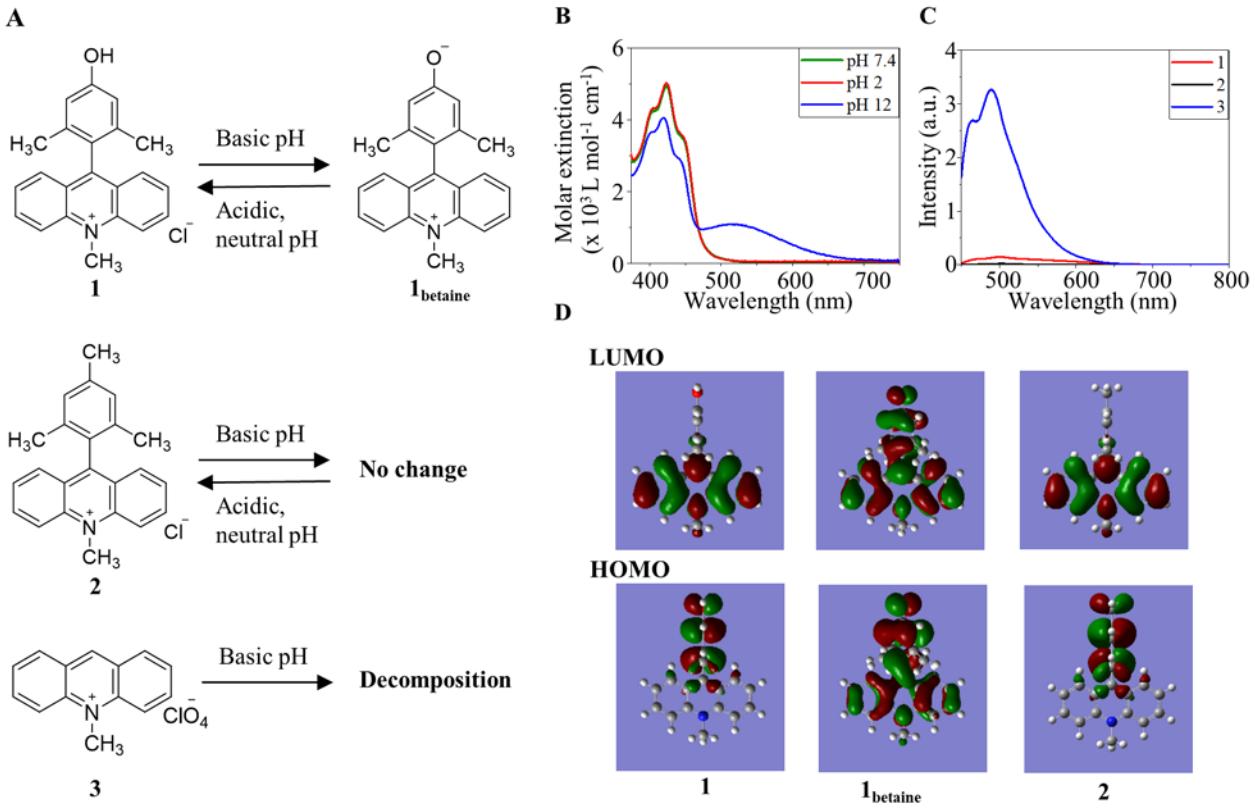

Figure 1. (A) pH-dependent structures of the molecules. (B) Absorption spectra of **1**. (C) Fluorescence spectra (λ_{ex}: 430 nm) of **1**, **2**, **3** at pH 7.4. (D) HOMOs and LUMOs of **1**, $\mathbf{1}_{betaine}$ and **2**, obtained by the DFT calculation at UB3LYP-D3/6-31G* level of theory. The chloride ion was omitted for the simplification of the calculations.

Results and Discussion

Absorption and fluorescence properties of 1 and 2

In this work, we investigated the PTE observed in a novel acridinium based electron donor-acceptor dyad, **1** and two reference molecules, **2** and **3** (Figure 1A). The detailed synthesis of **1** is provided in the supporting information. **2** was prepared using a procedure previously reported by our group,[15] and **3** was used as purchased.

Figure 1B shows the absorption spectra of **1** as the representative of the acridinium based molecules **1**-**3**. **1**-**3** show similar characteristic absorption band around 430 nm, which is mainly derived from the acridinium moiety (Figures 1B and S1). Meanwhile, pH-dependent spectral changes were observed at high pH as 12 for **1** and **3** (Figures 1B and S1). It is reported that the 9-position unsubstituted acridinium derivatives such as **3** are reactive towards the nucleophilic addition because the 9-position tends to be electron deficient.[17] As the result, the reaction of **3** with OH^- may proceed at pH 12, whereas **3** decomped at the basic pH, as reported in the literature.[17] In sharp contrast, **1** and **2** are stable at pH 12. This is due to the hindrance around the 9-position of the acridinium moiety by the closely located two methyl groups in the benzene ring.[3a] Although the absorption spectrum of **1** is pH-dependent, the change is reversible with changing the pH in between 2-12 (Figure 1B). At pH 12, **1** can be deprotonated to form a betaine structure, $\mathbf{1}_{betaine}$ (Figure 1A) in which pKa is determined at 9.2 by the titration experiments (Figure S2). **1** predominantly absorbs the light in UV-blue region (extinction coefficient: 4.46×10^3 L mol^{-1} cm^{-1} at 430 nm), whereas $\mathbf{1}_{betaine}$ absorbs the UV-blue light and the light between 480-700 nm. (extinction coefficients: 3.30×10^3 L mol^{-1} cm^{-1} at 430 nm, and 1.04×10^3 L mol^{-1} cm^{-1} at 530 nm). In the DFT calculations, HOMO and LUMO of **1** and **2** are found to be dominant on the donor and acceptor acridinium moieties, respectively (Figures 1D and S3). And there is no delocalization of the molecular orbitals in **1**. However, in the betaine-form, the HOMO and LUMO are extensively delocalized over the entire molecular skeleton. The information from DFT analysis is consistent with the observed absorption spectra showing characteristics of the acridinium moiety, which rule out any ground-state charge-transfer interaction between the donor and acceptor parts in the pristine state (**1**). Meanwhile, $\mathbf{1}_{betaine}$ shows the delocalization of HOMO

and LUMO, which leads to the changes in the absorption spectrum, showing a new peak around 530 nm (Figure S4). The expansion of the absorption of **1**$_{betaine}$ to the longer wavelength considered as an important feature to achieve the efficient enhancement of the PTE.

Figure 1C shows the fluorescence spectra of **1**-**3**, which provide insights into the transient pathways in the photoexcitation. It is reported that the fluorescence quantum yield of **3** is unity in phosphate buffer (pH 7.4).[18] The drastic fluorescence quenching observed in **1** and **2** relative to **3** suggests photoinduced intramolecular electron transfer (eT) followed by nonradiative deactivation. The thermodynamic feasibility of the eT between the donor and acceptor units was verified by estimating the free energy change of eT, according to eq. 1[20];

$$\Delta G = E_{ox} - E_{red} - E_{0,0} \qquad \text{(eq. 1)}$$

where, E_{ox} is the first oxidation potential of the donor moiety, and E_{red} is the first reduction potential of the acceptor, and $E_{0,0}$ is the zero-zero transition energy. The redox potentials of the compounds were determined by cyclic and differential pulse voltammetry. The obtained redox potentials are shown in Table 1, and the first oxidation and reduction potentials respectively arise from the oxidation of the donor moiety and reduction of the acceptor moiety, based on the literature[19] and our DFT calculations as shown in Figure 1D. Consequently, the free energy change of eT in **1** is significantly negative, which validates the thermodynamic feasibility of the photoinduced intramolecular eT. **2** is reported to show photoinduced eT.[15] The DFT calculations also supported the feasibility of the photoinduced intramolecular eT in which the orbital distribution of **1** and **2** are preferable to facilitate the intramolecular eT, that is the dominant distributions of HOMO and LUMO on the donor and acceptor moieties respectively (Figure 1D).

Table 1. The first redox potentials, zero-zero transition energy, and the free energy change of eT in **1** in aqueous solutions [a]

pH	E_{red}	E_{ox}	$E_{0,0}$	ΔG_{ET}
4	-0.59	0.43	2.69	-1.67
7.4	-0.60	0.50	2.69	-1.59

[a] Values of redox potentials are given in volts relative to $Fc^{0/+}$ redox couple and were obtained from differential pulse voltammetry. Conditions: a glassy carbon electrode as the working electrode, a platinum wire as the counter electrode, and $Ag/AgNO_3$ electrode as the reference electrode.

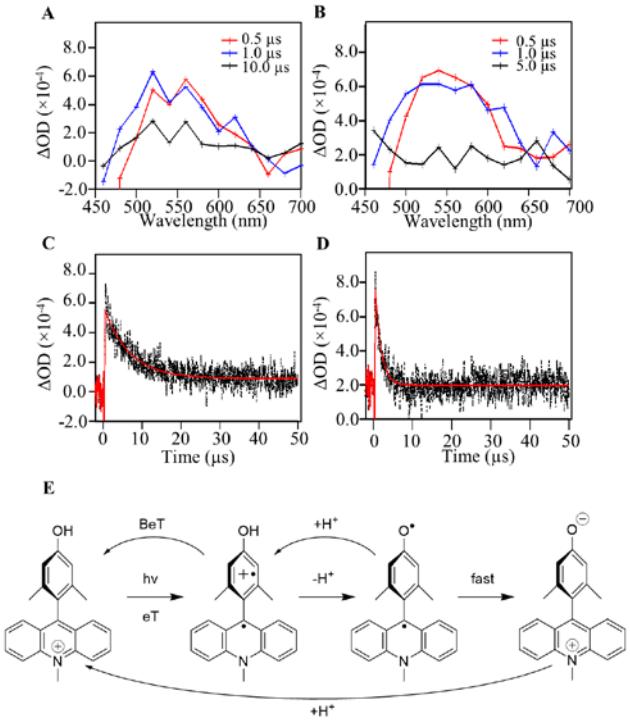

Figure 2. Nanosecond-transient absorption spectra of **1** in aqueous solutions at (A) pH 7.4 and (B) pH 6. Decay profiles at 540 nm arising from the **1**$_{betaine}$ in aqueous solutions at (C) pH 7.4 and (D) pH 6 with the observed signals (black dot) and mono-exponential fitting curve (red line). △OD denotes a change in optical density. (E) The feasible scheme of the photoinduced eT and subsequent deprotonation/protonation leading to the formation of **1**$_{betaine}$ from **1**. BeT: Back electron transfer.

The nanosecond transient absorption spectra were recorded for **1** and **2** to observe the individual photoinduced long-lived intermidiates in the aqueous solutions. Figure 2 shows the transient absorption spectra of **1** at pH 7.4 and pH 6. After a pulsed laser excitation at 430 nm, **1** showed a peak centered at 540 nm as a long-lived component with a half-life of 6.6 μs at pH 7.4 (Figures 2A and 2C). This peak shape resembles the peak obtained from the differential spectra between **1** and **1**$_{betaine}$ (Figure S4), which corresponds to the characteristic peak of betaine. This long-lived component (t ~ 6.6 μs) is attributed to **1**$_{betaine}$. As further evidence for the photo-triggered formation of **1**$_{betaine}$, pH dependence of the half-life of the component was examined. At pH 6, the signal shows the decay with half-life of 1.5 μs (Figures 2B and 2D), and at pH 5 no signal was observed in the available timescale in the current condition of our apparatus (>500 ns), where the signal of **1**$_{betaine}$ can be obscured by the luminescence from the compound (Figure S5). The betaine-form can be evolved as the result of the photoinduced intramolecular eT (Figure 2E), which is followed by deprotonation of the phenolic OH group, and a fast intramolecular eT could not be observed in the time-resolution of our experimental apparatus (>10 ns). Generally, phenolic OH groups lead to deprotonation when the adjacent aromatic ring is oxidized by the one-electron oxidation process. It is reported that a compound with a structure similar to **1**,[20] comprising an acridinium and phenolic moieties, can be deprotonated with illumination and act as a photoacid. These results support the photoassisted formation of **1**$_{betaine}$, which can

return to **1** by a faster protonation at a lower pH of the proton-rich environment. The photogenerated $\mathbf{1}_{betaine}$ can get converted to **1** by a faster protonation at a lower pH of the proton-rich environment. Meanwhile, after a laser excitation at 430 nm, **2** showed a characteristic peak centered at 500 nm at pH 7.4 (Figure S5). The shape and half-life of the peak (t ~ 35 μs) are identical to those arising from the charge-shifted state of **2** ($\mathbf{2}^{CS}$), where one-electron oxidized mesitylene moiety and one-electron reduced acridinium moiety are formed, as in the literature (t ~ 35 μs),[14] confirming the occurrence of photoinduced intramolecular eT, forming a charge-separated state in **2**. Consequently, we concluded that both **1** and **2** can form different long-lived photogenerated species, $\mathbf{1}_{betaine}$ and $\mathbf{2}^{CS}$, and the additional photoexcitation of these species is possible.

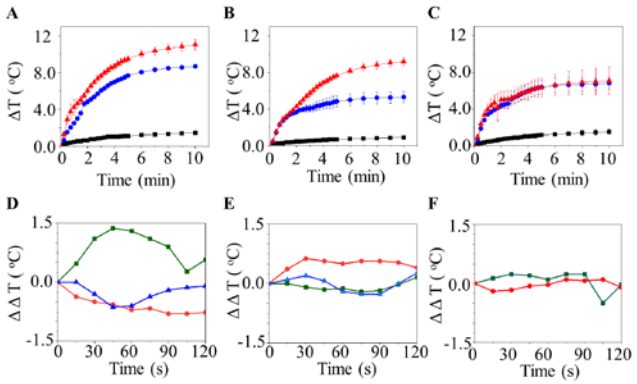

Figure 3. The photothermal responses induced by (A) **1**, (B) **2** and (C) **3** at pH 7.4 due to the excitation with the blue light (420-440 nm, 140 mW cm^{-2}) (blue circle), a Xenon lamp (>480 nm, 440 mW cm^{-2}) (black square), or simultaneous excitation with both the light sources (red triangle). The effective photothermal effect which is enhanced by the dual photoexcitation of (D) **1**, (E) **2** and (F) **3** at pH 7.4 (green square), pH 2 (red circle), and pH 12 (blue triangle). Data of **3** at pH 12 is not shown because **3** decomposes at pH 12.

pH-Dependent photothermal effect (PTE) by dual photoexcitation.

PTE is one of the fundamental and vital approaches of photoenergy conversion. The PTE refers to the liberation process of the photoexcitation energy by an agent in the form of heat to the external matrix. The molecules in the excited state adopt several pathways of relaxation. The nonradiative relaxation pathways lead to the evolution of the PTE by organic molecules.[4d]

The long-lived photogenerated species $\mathbf{1}_{betaine}$ and $\mathbf{2}^{CS}$ encouraged us to use them as a light-responsive heat emitter with enhanced light-harvesting ability owing to their expanded light absorption in the transient state. Thus, we investigated the PTEs of **1** and **2**, which can be enhanced by an additional photoexcitation of the long-lived $\mathbf{1}_{betaine}$ and $\mathbf{2}^{CS}$. For this purpose, we applied a dual photoexcitation technique using two individual light sources. One is blue light (420-440 nm LED, 140 mW cm^{-2}), to excite the molecule from its ground state and the other is yellow light (>480 nm Xe-lamp with a long pass filter, 440 mW cm^{-2}), to excite the long-lived photogenerated species. Both **1** and **2** do not have considerable absorption in the wavelength higher than 480 nm in their ground states, and $\mathbf{1}_{betaine}$ and $\mathbf{2}^{CS}$ absorb this region of the light with wavelength longer than 480 nm.

Figure 3A-C show the PTEs observed for **1**-**3** at pH 7.4 by the blue light (420-440 nm, 140 mW cm^{-2}), the yellow light (>480 nm, 440 mW cm^{-2}), or both at the same time which is denoted as "dual photoexcitation" in the present study. During the long period of illumination, up to 10 min, **1**-**3** showed significant increases of the temperature by the blue light illumination and the dual photoexcitation. In contrast, the yellow light illumination on **1**-**3** did not cause significant PTE. Among **1**-**3**, **1** showed the most substantial increase in the temperature up to 11.0 °C at 10 min (Figure 3A) by the dual photoexcitation, indicating high PTE by **1**. The photothermal conversion efficiency of **1** under the blue light illumination was determined using a monochromatic light source (446 nm diode laser, 75 mW cm^{-2}). The photothermal conversion efficiency of **1** was determined at 43 % (Figure S6). This value is sufficiently high as a model organic molecule for photothermal conversion.[21] Betaine-type molecules predominantly adopt a nonradiative relaxation pathway to liberate the excitation energy, which leads to the high efficiency of PTE.[21] To clarify the change of the temperature-induced by the additional excitation of the photogenerated species that is hereafter denoted as "the enhanced PTE", we constructed the differential plots between the temperature change by the dual photoexcitation and the simple sum of those by the blue light and yellow light excitations as a function of the time under photoexcitation. In other words, the positive values in Figures 3D-F reflect the enhanced PTE, which can be achieved only in the case of the dual photoexcitation. From Figure 3D, **1** shows considerably significant effects of the dual photoexcitation, and **3** does not show any enhanced PTE, as shown in Figure 3F.

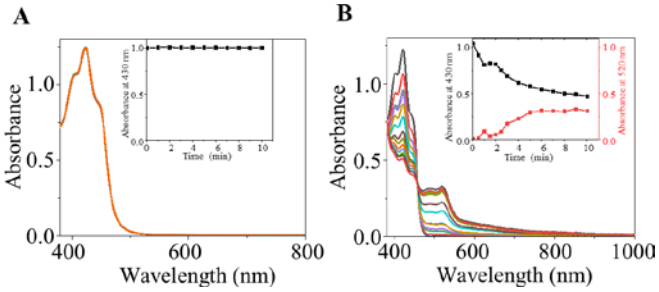

Figure 4. Absorption spectra recorded as a function of the time under the dual photoexcitation of (A) **1** and (B) **2** at pH 7.4. The insets show the changes in the absorbance at 430 nm and 520 nm as a function of the time under photoirradiation.

Interestingly, **1** exhibited outstanding stability during the illumination for a prolonged time (Figures 4A and S6), even 7 days after continuous photoillumination (Figure S8). Therefore, from the viewpoint of the pH-independent stability in the steady-state and the photoexcited states, **1** is the best candidate for the photothermal conversion with high durability and recyclability at various pH. In contrast, after the illumination with the blue light, **2** showed remarkable photodegradation (Figures 4B, S7, and S8). The decrease in the characteristic band around 430 nm of **2** suggests the decomposition of the acridinium moiety. The

increase in pH accelerated its degradation (Figure S7). The decomposition can be attributed to the nucleophilic attack of OH^- to the photoexcited acridinium.[22] It was reported that the intermolecular reactions of analogous acridinium derivatives compete with intramolecular eT.[3a] At low pH, such as pH **2**, this transformation is decelerated due to the low concertation of OH^- where the hydroxylation process is suppressed, making the compound photostable at lower pH (Figure S7). Therefore, we verified that the acidic pH is necessarily required to use **2** and its derivatives as a highly efficient photocatalyst in the aqueous medium.

It is noteworthy that **1** displayed a significant response to the dual photoexcitation at pH 7.4 at which $\mathbf{1}_{betaine}$ is formed with appreciable lifetime after the blue light illumination (Figures 2A and 2C). **1** showed the remarkable enhanced PTE up to 1.4 °C within one min of the dual photoexcitation (Figure 3D). The increase in the thermal response corresponds to 37 % enhancement of the PTE (3.8 °C) by **1** at the particular time point. The enhanced PTE observed in **1** can be explained by the proposed mechanistic pathway, as depicted in Scheme 1. At pH 7.4, **1** is in the protonated form in the ground state. By photoillumination **1** with the blue light, an intramolecular eT from the donor to the acridinium acceptor occurs. Subsequently, the OH group undergoes deprotonation and fast intramolecular eT(BeT) from the acridinium moiety to the benzene ring to form $\mathbf{1}_{betaine}$ with appreciably long lifetime, 6.6 μs at pH 7.4 (as observed in the nanosecond transient absorption spectra: Figure 2). Since $\mathbf{1}_{betaine}$ has an optical absorption in the 480-700 region, further excitation of the photogenerated $\mathbf{1}_{betaine}$ by the yellow light is possible, triggering the enhanced PTE. One reason for the moderate value of the enhanced PTE is that $\mathbf{1}_{betaine}$ itself absorbs the blue light (around 430 nm). Therefore, $\mathbf{1}_{betaine}$ can also generate heat solely with blue light illumination, which causes moderately enhanced PTE with the yellow light illumination.

The photothermal effect showed significant pH dependency. The enhanced PTE was amiss in **1** at acidic pH (pH 2), at which the lifetime of the photogenerated $\mathbf{1}_{betaine}$ can be very short (Figure 3D). At basic pH (pH 12), $\mathbf{1}_{betaine}$ is spontaneously generated without the blue light illumination, and thus the enhanced PTE was not observed. The enhanced PTE exhibited by **1** showed substantial power dependency of the blue light. The PTE conversion efficiency can be improved with the increase in illumination power (Figure S9). These results imply that the PTE efficiency of **1** can be magnified by applying a proper condition, such as pH, and the induced power of the light for future practical applications.

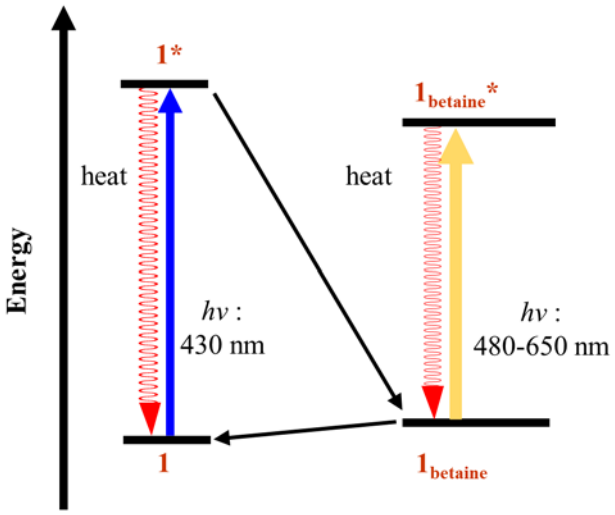

Scheme 1. Energy level diagram showing the formation of betaine and the subsequent irradiation, leading to the enhanced PTE.

Conclusions

We report the unique PTE caused by the acridinium-based compounds **1**, **2**, and **3**. **1** showed a pH-dependent formation of the photogenerated betaine $\mathbf{1}_{betaine}$ which absorbs the light in the 480-700 nm range, which was verified by ns-transient absorption studies, and DFT calculations. Meanwhile, **2** showed a colossal photodegradation at the neutral and basic pH, limiting its recyclability for photoenergy conversion. **1** showed astounding photostability with the enhanced PTE. The photothermal conversion efficiency of **1** was found to be 43% with the blue laser illumination, and the dual photoirradiation boosts the PTE. The present study provides useful information to design and synthesise of molecules and further improve the light harvesting properties by the additional excitation of the photogenerated species. This work opens up a promising strategy for utilizing the unique light absorption properties of photogenerated species to achieve efficient conversion of light energy into thermal energy.

Experimental Section

Materials

All chemicals used in the study were synthetic or analytical grade and used as received unless otherwise stated. 10-methylacridinium perchlorate, 9-mesityl-10-methylacridinium perchlorate, 10-methyl acridone were obtained from Tokyo Chemical Industry (Japan). Solvents such as anhydrous tetrahydrofuran, anhydrous dichloromethane, methanol, acetonitrile, and deionized water were obtained from FUJIFILM Wako Pure Chemical Corporation (Japan). Phosphate buffer solution at pH 7.4 was used for the studies. For acidic pH, aqueous hydrochloric acid and for the basic pH aqueous NaOH solution was used.

General

Absorption and fluorescence spectra were recorded using a UV-Visible spectrophotometer (Evolution 220, ThermoFisher Scientific) and a fluorescence spectrophotometer (Spectrofluorometer FL4500, Hitachi). ^{1}H and ^{13}C NMR spectra were measured using an Agilent Unity INOVA 500 spectrometer. FT-IR spectra were recorded on a JEOL FT/IR 660Plus spectrometer. High-resolution ESI mass spectra were obtained with ThermoFisher Scientific Exactive (ESI).

Synthesis

The synthesis and characterization of **1** are provided in the supporting information. **2** was prepared according to the reported procedure.[15]

DFT calculations

Geometries of **1, 1$_{betaine}$** and **2** were optimized using the Gaussian 09 Revision D.01 program[23] with the B3LYP[24] functional with the D3 version of Grimme's dispersion with the original D3 damping function[25]. The 6-31G(d)[26] basis set was used.

Electrochemical Measurements

Electrochemical measurements were performed using a BAS ALS 630 electrochemical analyzer. Redox potentials were determined by differential pulse voltammetry (DPV) in phosphate buffer. A glassy carbon (3 mm diameter) working electrode, Ag/AgCl (sat. KCl) reference electrode, and Pt wire counter electrode were employed. Ferrocenium hexafluorophosphate was used as the internal standard.

Nanosecond transient absorption measurements:

Nanosecond transient absorption measurements were carried out using the laser system NanoSpeK TSP-2000 (Unisoku Co., Ltd., Osaka, Japan). Solvents were deaerated by argon bubbling for 10 min before measurements. A solution containing a sample was excited by a Panther OPO pumped by a Nd:YAG laser (Continuum SLII-10, 4-6 ns fwhm), and the photodynamics were monitored by continuous exposure to a xenon lamp (150 W) as a probe light and a photomultiplier tube (Hamamatsu 2949) as a detector. The instrument response function (IRF) for this system is less than 10 ns.

Photothermal effect (PTE) studies.

PTE of **1**, **2**, and **3** were evaluated as follows. The light sources were a Xenon lamp with a bandpass filter (>480 nm at 440 mW cm^{-2}) and a blue LED (420-440 nm, 140 mW cm^{-2}). The sample solutions whose absorbance at 430 nm are set to be 1.00 were taken in a 2 mm-path glass cuvette. Sample solutions were irradiated by the individual light or by simultaneously both the light sources on the same face of the cuvette to achieve synchronous excitation of the molecule by both the blue and yellow lights. A digital thermometer was used to analyze the temperature response, and the sensor was dipped in the sample solution meticulously by avoiding the direct illumination. Each experiment was repeated 4 times to avail the standard deviation. From the data obtained, we analyzed the differential thermal response by dual wavelength excitation by subtracting the sum of individual wavelength response from the thermal response due to simultaneous excitation with both the light source.

Acknowledgments

D. S. acknowledges the English Program of Environmental Earth Science (EPEES) and scholarships by the Japan Student Services Organization (JASSO). Y.T. thanks to Prof. H. Imahori and Prof. A. Frube for the supports to measure transient absorption spectra. We acknowledge the Dynamic Alliance for Open Innovation Bridging Human, Environment and Materials.

Keywords: Photochemistry • Electron transfer • Donor-acceptor systems • Betaines • Energy conversion

[1] a) G. J. Hedley, A. Ruseckas, I. D. W. Samuel, *Chem. Rev.* **2017**, *117*, 796-837; b) H. Spanggaard, F. C. Krebs, *Sol. Energy Mater. Sol. Cells.* **2004**, *83*, 125-146; c) A. Hagfeldt, M. Grätzel, *Acc. Chem. Res.* **2000**, *33*, 269-277; d) A. Mishra, P. Bäuerle, *Angew. Chem. Int. Ed.* **2012**, *51*, 2020-2067; e) M. Grätzel, *J. Photochem. Photobiol. C. **2003**, 4,* 145-153; e) E. Bundgaard, F. C. Krebs, *Sol. Energy Mater. Sol. Cells.* **2007**, *91*, 954-985.

[2] a) M. R. Wasielewski, *Chem. Rev.* **1992**, *92*, 435-461; b) A. J. Bard, M. A. Fox, *Acc. Chem. Res.* **1995**, *28*, 141-145; c) J. H. Alstrum-Acevedo, M. K. Brennaman, T. J. Meyer, *Inorg. Chem.* **2005**, *44*, 6802-6827; d) D. Gust, T.A. Moore, A.L. Moore, *Acc. Chem. Res.* **2001**, 34, 40-48; e) S. Fukuzumi, K. Ohkubo, T. Suenobu, *Acc. Chem. Res.* **2014**, *47*, 1455-1464; f) Y. Tachibana, L. Vayssieres, J. R. Durrant, *Nat. Photonics.* **2012**, *6*, 511-518.

[3] a) N. A. Romero, D. A. Nicewicz, *Chem. Rev.* **2016**, *116*, 10075-10166; b) L. Marzo, S. K. Pagire, O. Reiser, B. König, *Angew. Chem. Int. Ed.* **2018**, *57*, 10034-10072; c) S. Fukuzumi, K. Ohkubo, *Chem. Sci.* **2013**, *4*, 561-574; d) N.A. Romero, K.A. Margrey, N.E. Tay, D.A. Nicewicz, *Science* **2015**, *349*, 1326-1330; e) S. Shanmugam, C. Boyer, *Science* **2016**, *352*, 1053-1054.

[4] a) T. J. Dougherty, *Crit. Rev. Oncol. Hematol.* **1984**, 2, 83-116; b) S. B. Brown, E. A. Brown, I. Walker, *The Lancet Oncol.* **2004**, *5*, 497–508; c) D. E. Dolmans, D. Fukumura, R. K. Jain, *Nat. Rev. Cancer.* **2003**, *3*, 380-387; d) H. S. Jung, P. Verwilst, A. Sharma, J. Shin, J. L. Sessler, J. S. Kim, *Chem. Soc. Rev.* **2018**, *47*, 2280–2297; e) J. Chen, C. Ning, Z. Zhou, P. Yu, Y. Zhu, G. Tan, C. Mao, *Prog. Mater. Sci.* **2019**, *99*, 1–26.

[5] a) N. S. Lewis, *Science* **2012**, *798*, 798–801; b) G.W. Crabtree, and N.S. Lewis, *Physics today* **2007**, *60*, 37-42.

[6] a) G. D. Scholes, G. R. Fleming, A. Olaya-Castro, R. Van Grondelle, *Nat. Chem.* **2011**, *3*, 763–774; b) X. Feng, X. Ding, L. Chen, Y. Wu, L. Liu, M. Addicoat, S. Irle, Y. Dong, D. Jiang, *Sci. Rep.* **2016**, *6*, 1–13.

[7] J. Haimerl, I. Ghosh, B. König, J. Vogelsang, J. M. Lupton, *Chem. Sci.* **2019**, *10*, 681–687.

[8] L. Zhang, R. Li, B. Tang, P. Wang, *Nanoscale* **2016**, *8*, 14600–14607.

[9] W. O. Wray, T. Aida, R. B. Dyer, *Appl. Phys. B Lasers Opt.* **2002**, *74*, 57–66; b) G. M. Neelgund, A. Oki, *Mater. Chem. Front.* **2018**, *2*, 64–75.

[10] X. Song, Q. Chen, Z. Liu, *Nano Res.* **2015**, *8*, 340–354.

[11] a) B. Macht, M. Turrión, A. Barkschat, P. Salvador, K. Ellmer, H. Tributsch, *Sol. Energy Mater. Sol. Cells.* **2002**, *73*, 163–173; b) M. B. Upama, M. Wright, M. A. Mahmud, N. K. Elumalai, A. Mahboubi Soufiani, D. Wang, C. Xu, A. Uddin, *Nanoscale* **2017**, *9*, 18788–18797; c) M. Jørgensen, K. Norrman, F. C. Krebs, *Sol. Energy Mater. Sol. Cells*. **2008**, *92*, 686–714.

[12] A. C. Benniston, K. J. Elliott, R. W. Harrington, W. Clegg, *European J. Org. Chem.* **2009**, 253–258.

[13] V. Kharlanov, W. Rettig, *J. Phys. Chem. A* **2009**, *113*, 10693–10703.

[14] K. Ohkubo, K. Mizushima, R. Iwataa, S. Fukuzumi, *Chem. Sci.* **2011**, *2*, 715–722.

[15] Y. Takano, E. Hanai, H. Imahori, *Nanoscale* **2017**, *9*, 17909–17913.

[16] Y. Takano, T. Numata, K. Fujishima, K. Miyake, K. Nakao, W. D. Grove, R. Inoue, M. Kengaku, S. Sakaki, Y. Mori, et al., *Chem. Sci.* **2016**, *7*, 3331–3337.

[17] M. Adamczyk, Y. Y. Chen, P. G. Mattingly, J. A. Moore, K. Shreder, *Tetrahedron* **1999**, *55*, 10899–10914.

[18] J. Joseph, E. Kuruvilla, A. T. Achuthan, D. Ramaiah, G. B. Schuster, *Bioconjug. Chem.* **2004**, *15*, 1230–1235.

[19] S. Fukuzumi, H. Kotani, K. Ohkubo, S. Ogo, N. V. Tkachenko, H. Lemmetyinen, *J. Am. Chem. Soc.* **2004**, *126*, 1600–1601.

[20] G. Zhao and T. Wang, *Angew. Chem. Int. Ed.* **2018**, 6120–6124.

[21] a) X. Liu, B. Li, F. Fu, K. Xu, R. Zou, Q. Wang, B. Zhang, Z. Chen and J. Hu, *Dalt. Trans.* **2014**, 43, 11709–11715; b) M. Lan, L. Guo, S. Zhao, Z. Zhang, Q. Jia, L. Yan, J. Xia, H. Zhang, P. Wang and W. Zhang, *Adv. Ther.* **2018**, **1**, 1800077.

[22] M. Nakazono, Y. Oshikawa, M. Nakamura, H. Kubota, S. Nanbu, *J. Org. Chem.* **2017**, *82*, 2450–2461.

[23] Frisch, M. J., Trucks, G. W., Schlegel, H. B., Scuseria, G. E., Robb, M. A., Cheeseman, J. R., Scalmani, G., Barone, V., Mennucci, B., Petersson, G. A., Nakatsuji, H., Caricato, M., Li, X., Hratchian, H. P., Izmaylov, A. F., Bloino, J., Zheng, G., Sonnenberg, J. L., Hada, M., Ehara, M., Toyota, K., Fukuda, R.; Hasegawa, J.; Ishida, M.; Nakajima, T.; Honda, Y.; Kitao, O.; Nakai, H.; Vreven, T.; Montgomery, Jr., J. A.; Peralta, J. E.; Ogliaro, F.; Bearpark, M.; Heyd, J. J.; Brothers, E.; Kudin, K. N.; Staroverov, V. N.; Kobayashi, R.; Normand, J.; Raghavachari, K.; Rendell, A.; Burant, J. C.; Iyengar, S. S.; Tomasi, J.; Cossi, M.; Rega, N.; Millam, J. M.; Klene, M.; Knox, J. E.; Cross, J. B.; Bakken, V.; Adamo, C.; Jaramillo, J.; Gomperts, R.; Stratmann, R. E.; Yazyev, O.; Austin, A. J.; Cammi, R.; Pomelli, C. J.; Ochterski, W.; Martin, R. L.; Morokuma, K.; Zakrzewski, V. G.; Voth, G. A.; Salvador, P.; Dannenberg, J. J.; Dapprich, S.; Daniels, A. D.; Farkas, O.; Foresman, J. B.; Ortiz, J. V.; Cioslowski, J. and Fox, D. J. GAUSSIAN 09, Revision D.01; Gaussian, Inc., Wallingford CT, (2009).

[24] a) A. D. Becke, *Phys. Rev. A* **1988**, *38*, 3098. b) A. D. Becke, *J. Chem. Phys.* **1993**, *98*, 5648. c) C. T. Lee, W. T. Yang, R. G. Parr, *Phys. Rev. B* **1988**, *37*, 785. d) Francl, M. M.; Pietro, W. J.; Hehre, W. J.; Binkley, J. S.; Gordon, M. S.; Defrees, D. J.; Pople, J. A. *J. Chem. Phys.* **1982**, *77*, 3654.

[25] S. Grimme, J. Antony, S. Ehrlich, H. Krieg, *J. Chem. Phys.* **2010**, *132*, 154104.

[26] (a) G. A. Petersson, M. A. Allaham, *J. Chem. Phys.* **1991**, *94*, 6081. (b) G. A. Petersson, A. Bennett, T. G. Tensfeldt, M. A. Allaham, W. A. Shirley, J. Mantzaris, *J. Chem. Phys.* **1988**, *89*, 2193.

Entry for the Table of Contents (Please choose one layout)

Layout 2:

FULL PAPER

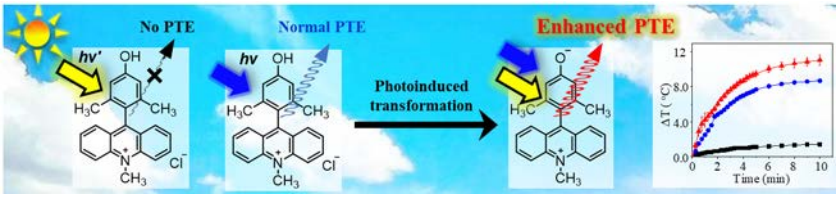

A long-lived photogenerated betaine from a donor-acceptor dyad molecule demonstrated an efficient light harvesting strategy. The photostable betaine which is generated by blue light illumination potentiates photothermal energy conversion efficiency of the dyad molecule because of the enhancement of the light absorbing property triggered by the illumination.

Devika Sasikumar, Yuta Takano, and Vasudevanpillai Biju**

Page No. – Page No.
Photoinduced Generation of the Betaine for Efficient Light-Harvesting and Photothermal Energy Conversion

Photochemistry • Electron transfer • Donor-acceptor systems • Betaines • Energy conversion